IEEE Access
Multidisciplinary | Rapid Review | Open Access Journal

Received September 29, 2020, accepted October 16, 2020, date of publication October 23, 2020, date of current version November 4, 2020.

Digital Object Identifier 10.1109/ACCESS.2020.3033290

Hornbill: A Self-Evaluating Hydro-Blasting Reconfigurable Robot for Ship Hull Maintenance

VEERAJAGADHESWAR PRABAKARAN[1], ANH VU LE[1,2], PHONE THIHA KYAW[1,3], RAJESH ELARA MOHAN[1], PRATHAP KANDASAMY[1], TAN NHAT NGUYEN[4], (Member, IEEE), AND MADHUKUMAR KANNAN[5]

[1]ROAR Laboratory, Engineering Product Development Pillar, Singapore University of Technology and Design, Singapore 487372
[2]Optoelectronics Research Group, Faculty of Electrical and Electronics Engineering, Ton Duc Thang University, Ho Chi Minh City 700000, Vietnam
[3]Department of Mechatronics Engineering, Yangon Technological University, Insein 11401, Myanmar
[4]Wireless Communications Research Group, Faculty of Electrical and Electronics Engineering, Ton Duc Thang University, Ho Chi Minh City 700000, Vietnam
[5]Brightsun Marine Pte Ltd., Singapore 639224

Corresponding author: Tan Nhat Nguyen (nguyennhattan@tdtu.edu.vn)

This work was supported in part by the National Robotics Programme under its Robotics Enabling Capabilities and Technologies (Funding Agency) under Project 192 25 00051, in part by the National Robotics Programme under its Robot Domain Specific (Funding Agency) under Project 192 22 00058, and in part by the Agency for Science, Technology and Research.

ABSTRACT Maintenance of ship hull involves routine tasks during dry-docking that includes inspection, paint stripping, and re-painting. Among those, paint stripping is always seen as harmful for human operators and a time-consuming task. To reduce human risk, cost, and environmental cleanliness, the shipping maintenance industries started using robotic solutions. However, most of such robotic systems cannot operate fully autonomous since it requires human in the loop to monitor the cleaning efficiency. To this end, a novel autonomous self-evaluating hull cleaning robot called Hornbill is presented in this paper. The proposed robot is capable of navigating autonomously on the hull surface and perform water jet blasting to strip off the paint coating. The robot is also enabled with a Deep Convolutional Neural Network (DCNN) based self-evaluating scheme that benchmarks cleaning efficiency. We evaluated the proposed robot's performance by conducting experimental trials on a metal plate under three different paint coatings. While performing the paint stripping task in every experimental trial, the self-evaluating scheme would generate the heat map that depicts the plate's cleanliness. The results indicate that the proposed self-evaluating system could successfully generate high accurate cleanliness heat maps in all considered scenarios, which simplifies the checkup process for paint inspectors.

INDEX TERMS Benchmarking blasting quality, hydro blasting, paint stripping, reconfigurable robotics, robotics for ship maintenance industry.

I. INTRODUCTION

Maintaining a smooth and foul free operation of ships involves a series of routine repair tasks. One such task is cleaning of ship hulls, which usually is done in dry-dock with the employment of different adapted methods like grit or water jet blasting, as shown in Fig. 1. Most of these ship hull cleaning activities focus on removing barnacles, paint, and rust, which are always seen as harmful for human operators and time-consuming tasks. The cleaning robots become popular in the model civilization; they are set to self-operate in both indoor [1], [2] and outdoor environments [3], [4]. By witnessing the evolution of robotization over the last few decades, the ship maintenance industry has shown great interest in deploying robots for hull cleaning tasks to reduce the risk of employing manual labor. Such an effort increases the number of robotic products that are being used for ship hull maintenance task, and it is expecting to grow at a Compound annual growth rate (CAGR) of 16.2 between the year 2018 to 2027 [5]. The thriving market players include HullBUG, Magnetic Hull Cleaner, Remora, RovingBAT, GreenSea Robotic Hull Cleaner, and Vertidrive. These robots are often equipped with both grid and water blasting types of equipment and can operate in both autonomous and semi-autonomous mode to clean the defined hull area. On the other hand, academic research

The associate editor coordinating the review of this manuscript and approving it for publication was Ehsan Asadi.

on ship hull cleaning robots continued to improve aspects of mechanism design, autonomy, human-robot, and multi-robot operation. For instance, Kang, Hoon *et al.* presented a pose estimation scheme using an optimal displacement sensor for a hull cleaning robot [6]. They validated the proposed algorithm on an identical driving platform and shown better results than an encoder. A similar positioning system for a hull cleaning robot is presented in [7]. This article describes a sensorial fusion model for a better 3d positioning of the robot in both the upper and inner surface of the water. Cassee, Kes proposes an ultrasonic based localization system that aids the hull cleaning robot to navigate autonomously with minimal error in pose [8]. The presented system predicts the upcoming wheel slippages concerning the ship hull's surface and adds the error to neglect it in the pose estimator functions. From the same lab, Steensma Bart contributes towards developing an obstacle avoidance framework for the hull cleaning robot [9]. The author used a forward-looking sonar method that can provide an acoustic image wherein the obstacles were detected. D. Souto *et al.* proposed a semi-autonomous hull cleaning system called lappa, which was designed in such a way to clean every nuke and corner [10]. Other similar works in floor suffface maintenance are presented in [11], [12]. Although numerous literature studies demonstrated the autonomous ability of ship hull cleaning robots, they mostly deal with underwater operations. One primary maintenance cleaning task that was never focused on in the previous works is paint stripping, which is usually done in dry-docking.

Concerning hull paint stripping robots, Xu *et al.* [13] presented an optimistic solution for designing a magnetic wheel of a grid blasting cleaning robot. The proposed robotic system can adapt to navigate on any curved surfaces in a ship hull. In another similar work, Wei Song *et al.* proposed a water blasting based hull cleaning robot with a permanent magnet adhesion system [14]. The author focused on designing a lightweight magnetic system to optimize the adhesion force while propagating in the curved hull area. For bigger ship, A. Iborra *et al.* proposes a family of the robot consisting of the large vertical tower attached with the two robotic platforms that can move in vertically [15]. The proposed system can perform a water blast to strip existing paint in a ship hull at a low cost. However, most of these platforms were operated manually using a remote control without any autonomous capability and always had human in the loop. A particular factor that lacks the autonomous deployment of a hull cleaning robot is the lack of monitoring of the cleaning efficiency, rectified with the supervised cleaning process. A viable approach to overcome this bottleneck in deploying an un-supervised hull paint stripping robot is to implement an advanced autonomous capability that can self-evaluate the cleaning performance.

Self-evaluation or self-supervising philosophies in robotic systems have been actively studied in the last two decades. After the advancement of artificial intelligence, this trend is increasing further in self-supervised localization, navigation, and manipulation. When it comes to cleaning, Ariyan M. Kabir *et al.* proposed a self-supervised robotics system to perform an efficient floor scrubbing task [16]. The proposed robotic system identifies the floor's cleanliness to optimize the cleaning parameters such as applied force, speed of scrubbing motor, and stiffness of the robot for achieving efficient cleaning. Joshua J. Yin *et al.* presented a self-supervised approach in a service robot cleaning task [17]. The proposed approach self-learn the deformation pattern of the material and optimize the cleaning parameters of the robot to perform effectively. In another work, Ariyan M. Kabir *et al.* introduced a novel self-evaluating strain cleaning robot [18]. The proposed robot could remove the strain in the curved surface by self-evaluating its position and orientation that is optimal for efficient cleaning. Some open-ended evaluation schemes were proposed for a reconfigurable cleaning robot in [19], [20]. Wherein the robot's coverage area was evaluated to choose a better morphology for maximizing the coverage. The interaction path planning to do cleaning and maintenance tasks is discovered in the works of [21], [22]. The aids of optimization in the path planning proved useful in finding the optimal navigation strategies for mobile robot [23], Although numerous studies in the literature demonstrate the advantage of self-supervising robotic systems in the cleaning task, they are primarily limited to lab space, often not tested in real-world scenarios. None of the above studies targeted ship hull paint stripping tasks, which presents significant research and development opportunities.

A novel autonomous self-evaluating hull cleaning framework for a robot called Hornbill is presented in this paper. Hornbill is developed under the principle of magnetic adhesion to navigate on the metallic hull surface. The proposed robot is equipped with water jet blasting components connected with a blasting machine that aids in stripping off the paint coating. The robot is also loaded with all necessary electronics that enable the self-evaluation of the paint stripping task. The significant challenges encountered during the development of our hornbill robot were its adhesion mechanism, the integration of waterjet blasting modules, autonomous navigation, and translating the theoretical design of self-evaluation into a workable system. This paper summarizes all these aspects and concludes with experimental results that validate the proposed robot and its self-evaluation system.

This paper is organized as follows: Section II introduces the mechanical design principles and Hornbill's system architecture. Section III presents the autonomy building blocks of Hornbill and discusses the robot's coverage path pattern. Section IV Introduces the learning-based self-supervising scheme and its network architecture. Section V presents the detailed of our experimental setup and methods and analyzes the results of validating the paint stripping performance of the Hornbill robot. Finally, section V concludes this study and discusses future research directions.

II. HORNBILL ROBOT SYSTEM ARCHITECTURE

The proposed hornbill robot (Fig.2) is explicitly designed to navigate on a vertical metal surface with zero tolerance in

FIGURE 1. ShipHull surface with corrosion and blasting by Hornbil.

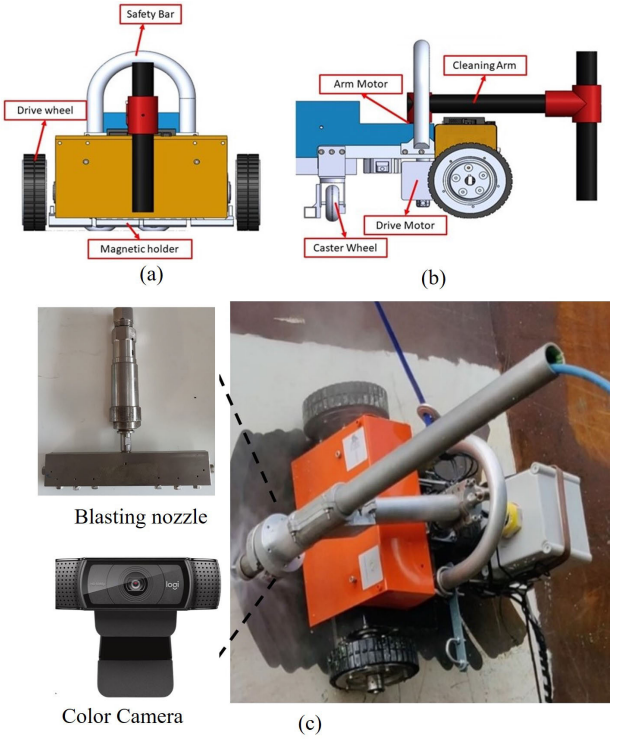

FIGURE 2. The Hornbill robot, (a) Front view design, (b) Side view design, (c) Reconfigurable Robot platform with Blasting and Camera Modules.

slippages. Our robot architecture has also been carried out, taking into account that its primary mission is hydro blasting with a pressure maximum of 3000 bar. To cover the predefined workspace during paint stripping and benchmarking, the Hornbill robot will flow the zigzag trajectory defined as a global planner. To change trajectories of the robot based on the velocity change in the differential drive, our robot uses the move base framework with the point pursuit local planner the service provided by ROS to fulfill the trajectory tracking.

A. LOCOMOTION DESIGN

The proposed robot's locomotion system was developed under the principle of differential drive, which aids in achieving smooth navigation. The locomotion system was mounted on an aluminum chassis with a dimension of 100mm x 250mm x 500mm. Since the differential drive is a well-established mechanism mobile robotic platform, we implemented the same on our system. The locomotion system consists of two 48 volt and 400 watts brush-less dc motor coupled with a 100:1 planetary gear reducer. This high torque motor smoothly drives the whole robot on the vertical surface against the robot's powerful adhesion force. Other than locomotion, our robot is equipped with One 24 volt 100 Watts brushless dc motor coupled with 100:1 planetary gear reducer to actuate the arm, which does the paint stripping. These motors have their internal electromagnetic braking system, which helps hold the robot's position and avoids the free rotation when the robot is pointing vertically.

Apart from motors and the locomotion system's main ingredient, the wheel is more critical in reducing the slippage for the robot while climbing. This wheel's major periphery is the rubber tread casted according to the specific hardness to reduce the slippage and increase the rolling coefficient of friction. The mold for the rubber tread is 3D printed using Selective Laser Assistive (SLA) method shown

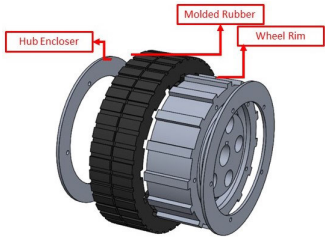

FIGURE 3. Drive wheel.

in Fig.3. This wheel tread has the hardness of 80A according to the standard. The main hub is CNC milled using aluminum material to have lesser weight. Apart from this, two polyurethane swivel caster wheels are connected with the chassis to increase stability, and it allows the robot to turn freely without any drag force on the wheel. The total weight of the robot goes up to 45 kg.

1) KINEMATIC LOCOMOTION SYSTEM

A mobile robot has 6 degrees of freedom (DOF) expressed by the pose: $(x, y, z, Roll, Pitch, Yaw)$. It is composed of two parts: the position = (x, y, z) and the attitude = $(Roll, Pitch, Yaw)$. For a Hornbill robot on a two-dimensional ship hull surface, the 2D pose (x, y, yaw), where yaw denotes the heading, is sufficient to describe its motion. With differential drive, the direction of motion is controlled by separately controlling speeds velocity of the left v_l and right v_r wheels, respectively. Based on inverse kinematic by the differential

drive module, the speed of each robot wheel be generated through the motor driver. The distance between 2 wheels of the robot wheel based w_b and robot wheel radius w_r in the inverse kinematic of the differential drive model is 0.5 m and 30 cm, respectively. The equations 1, and 2 are used to drive the velocity of the left and right wheel from the linear velocity l_v on the x-axis and angular velocity a_v on yaw orientation. In the Hornbill robot, we use the motors with the built-in precise speed controller from the Oriental branch.

The commanded velocity is generated online based on the deviation between the current robot location and goal location to control the robot adaptively to follow the pre-defined trajectory. We set the maximum linear and angular robot speed to 0.1 m/s and 0.2 rad/s, respectively. The robot location, including the current position and heading in the global frame, is the control loop input.

$$v_l = (l_v - a_v * W_b)/2.0)/W_r \quad (1)$$

$$v_r = (l_v + a_v * W_B/2.0)/W_r \quad (2)$$

B. MAGNETIC ADHESION SYSTEM

For the proposed robot, we used the magnetic adhesion principle to achieve the climbing ability on a ship hull. The robot is equipped with ten N52 grade Neodymium magnets at the bottom of the robot chassis. Each magnet has a dimension of 100 mm x 25 mm x 25 mm. The magnets are placed in four different parts of the chassis, which is shown in Fig.4a. Two sets of magnets were placed near the left and the right wheels, giving more force to ensure the friction. Similarly, we had four magnets at the center of the chassis, which gives enough force for the robot to keep the adhesion against the back-pressure during high-pressure water blasting. We attached one more magnet by splitting it into half to place it near the caster wheel, which gives more stability to the robot during locomotion.

All these magnets were placed in a magnetic holder that maintains the height of 8mm from the steel plate to avoid obstacles in the ship hull. The magnets are placed nearer to the wheel to increase the traction. We reduced the number of magnets even though we had the provision to reduce the robot's overall weight and increase the system's efficiency. Besides, 10 microns of three-layer Ni-Cu-Ni coating provided the necessary resistance to corrosion. The magnets exert a pull force of 138.25 kg normal to the steel plate. The pull force of the magnets varies according to the distance between the magnets and the steel plate. The force vs. air gap characteristic of robot magnets by The Special Finite Element method in Solidworks is shown in Fig.4b.

We quantify the stability of robot motion in terms of statics and dynamic criteria by setting the robot to clear the pairs of waypoints with defined paths in different directions, including horizontal, vertical, diagonal lines on the ship hull surface. We verify that the adhesion of magnetic panels can hold the robot, and the robot can keep track of the defined trajectories.

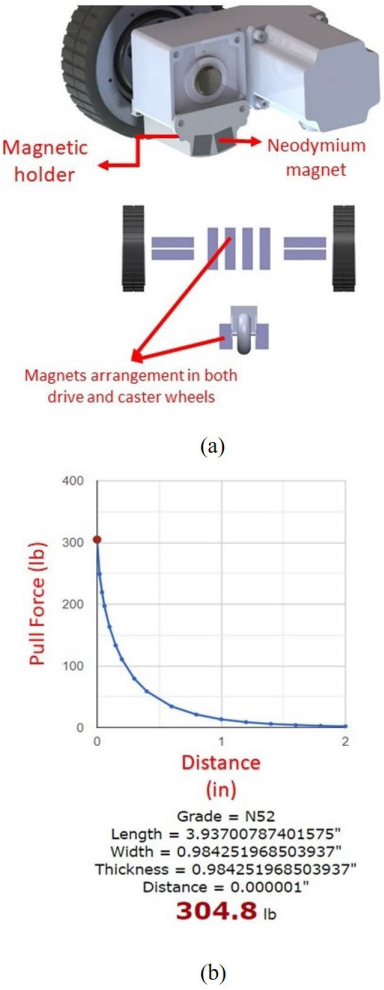

FIGURE 4. Magnets locations of magnets and the graph for realtion of force and magnet air gap.

C. WATER BLASTING SYSTEM

The concerned robot is designed to carry multiple functional payloads. However, this article focuses on the application of Hydro-blasting and benchmarking. The primary function of hydro blasting is to remove the paint, rust, and biofouling from the ship hull. A high-pressure non-abrasive hydro blasting was used to swipe barnacles from the ship hull surface. The nozzles types are selected basing on the debris type the thickness of the old paint layer. The paint sweeping uses the nozzle set with four 0.30mm diameter headers or two 0.40mm diameter headers, as shown in Fig.2c.

The paint removal setup from the steel plate includes a hydro-blasting machine powered by 440 V AC power supply, the shielded hose which carries high-pressure water, a safety valve for emergency cutoff, and a robot mounted with nozzle and other control accessories. Cleaning is initiated by the water entering into the hydro blasting machine where the machine pumps out the water with 2400 bar pressure through a human-operated safety valve to the nozzle mounted on to the robot arm.

D. ELECTRONIC AND POWER SYSTEM

When it comes to power and electronics architecture, we always used a tethered connection between the robot and the base station. The base station places all our critical equipment, consisting of an industrial PC, Monitor, power supply, and joystick controller. The maximum cable length between the base station and the robot is 100m, consisting of power cable and data cable. We separated the power source as 43v and 24v dc, which powers the locomotion motor and the arm motors subsequently. Also, the 24v DC is given to a 5V DC regulator, which powers the USB extender module. For the power source, we used a benchtop 220v AC to dc converter with two channels. In the base station, we equipped with an Industrial PC with a dedicated GPU that acts as a central processor for the hornbill robot. There are mainly two input signals that come to the PC, one is from the wireless joystick controller, and the second one is the data signal from the robot.

On the robot side, the components are divided into locomotion and autonomy peripherals. For the locomotion, the robot is housed with a set of 48V and one 24V motor driver, which controls both mobile and arm motor. These drivers are also responsible for receiving the motor's encoded data and passing it back to the main PC. All the motor drivers use RS485 communication protocol to communicate with the PC. Concerning the autonomy peripherals, we housed a monocular Logitech C920 camera, which is mounted at the backside of the robot that is used to get the video frames to classify the cleanliness after paint striping. The camera's technical specs are provided as follows: Full HD video recording up to 1920 x 1080 pixels, Built-in automatic noise reduction, Video compression, high definition, autofocus, low light mode features. We use the ROS USB cam package to stream the raw RGB data from the camera in real-time. To know the orientation of the robot on the vertical surface, we fixed a vectorNav absolute IMU. Also, we used beacons to know the robot's 3D position on the metal surface, which is critical for the robot to perform autonomous navigation. All these autonomous related sensors are attached in a USB along with the motor driver's RS485 to USB cable. The USB hub is then connected to a USB extender module, which extends the communication up to 100m via Ethernet cable. The Ethernet cable then converts back to the USB protocol at the industrial PC's end. The system overview is shown in Fig.5.

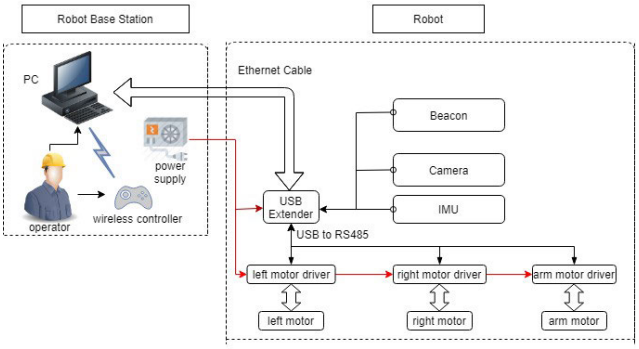

FIGURE 5. Hornbill system block diagram.

III. HORNBILL AUTONOMY BY SENSOR FUSSION

The developed robot can be operated in both manual and autonomous modes. For manual mode, we used an industrial radio-controller, which consists of a joystick and buttons. The radio-controller receiver is attached to the base station (Master-PC), which receives the input signals and converts them as numerical commands. These commands were then passed to the velocity controller to issue command velocity for the robot actuators. Mostly the manual control is used at the point of deployment to position the on the hull surface. Once the human operator thinks that the robot is in a correct position to perform autonomous cleaning, then the operator will press the specific button on the radio-controller to activate the autonomous mode.

In order to achieve autonomous propagation, it is critical to obtain an accurate robot's position on the hull surface. Conventional approaches estimating the global position of the robot are Lidar based simultaneous localization and mapping SLAM [24] and visual SLAM [25] and sensor fusion localization [26] and feature tracking [27]. These methods derive the features of objects inside the working environment to estimate the global location. Since the Hornbill robot performs an open water jet blasting, the traditional approaches would fail to get the coordinates since the feature is not accurate. To overcome these drawbacks, The Hornbill leveraged an ultrasonic-based beacon system that can provide an accurate robot position. The positioning system consists of a network of stationary beacons that are interconnected through radio waves. A mobile beacon with an inbuilt IMU sensor can be localized within this network at very high accuracy under the line of sight condition with stationary beacons. By sensing the reflective ultrasonic waves between the beacon set, the mobile beacon mounted on the robot base frame determines its relative location within the predefined boundary of static beacons. These 3D coordinates are converted into ROS [28] 3D pose messages and advertised as a topic named hedge_odom.

The UWB system only provides the 3D location x, y, z, and data noise happen during realtime operation. To overcome the kidnapping issues of robot localization, we need absolution orientation sensor data and another rotary odometry source. We used the Extended Kalman filter robot location package proved by ROS with multiple input sensors [29] to acquire the filtered odometry data. To address these requirements, we integrated the wheel encoder data from 24V DC motor drivers defined as whell_odom topic and 9 DoF orientation data defined as IMU topic from the industrial-grade IMU named VectorNa Vn-200 with the hardware-based noise cancelation. After factory calibration, the IMU provides the absolute 9 DOF orientation respecting to the North, East, Down fame. Note that the calibration parameters are stored inside

the IMU ROM, and there is no need to do the re-calibration processes after power off. The raw IMU and wheel_odom and hedge_pose are fed to the robot-localization package, which uses EKF to eliminate the sensor noise.

The values of process noise covariance (15×15 matrix with diagonal value indicate the noise we add to the total error after each prediction step) are turning based on the experimental trials and input sensor characteristics. The better the omnidirectional motion model matches the robot system, the smaller these values can be. If the system finds that a given variable is slow to converge, we increase the process noise covariance diagonal value for the variable in question, which will cause the filter's predicted error to be larger, which will cause the filter to trust the incoming measurement more during the correction. Since the position of beacon and orientation form the IMU are industrially reliable, the position x, y rely more on the beacon system, and the *yaw* value relies more on IMU; on the other hand, the velocity v_x and v_y is more based on the wheel odometry.

The ROS based sensor fusion flow is shown in Fig.6(top). The global and local planners use the filtered robot location to generate the appropriate execution commands during robot navigation on the ship hull.

When the autonomy mode is activated, the system will first generate a global path. Since we consider the paint stripping process as an area coverage task, we implemented a traditional zigzag pattern [30] as a global path. The global trajectory will be generated within a specified length and height, which could be assigned by the human operator. The generated path is used by the local path planner that generates the velocity commands for the actuators to execute the coverage. Fig.6(bottom) presents the robot operation on the ship hull. The paint stripping process is implemented in the predefined distance. After navigating 15 cm distance, the robot will stop until the robot arm module finished rotation one revolution. At each cycle of the robot arm, the water pressure by hydro blasting will sweep a arc shape with a diameter of 22cm. The process will continue while the robot follows the zigzag pattern until the area specified by operators is covered entirely.

IV. SELF-EVALUATING SCHEME

A. TRANSFER LEARNING USING INCEPTION v3

The self-evaluating algorithm estimates the level of cleanliness on the ship hull surface throughout the hornbill robot's paint stripping process. A GoogleNet Inception v3 CNN model with 48 laypers [31] that was pre-trained on approximately 1.28 million images (1,000 object categories) from the 2014 ImageNet Large Scale Visual Recognition Challenge [32] is applied, and retrain with our collected dataset using transfer learning [33]. Google's Inception v3 CNN architecture with 93.33% accuracy is the top-five object classification benchmark on the 1,000 object classes (1.28 million images) of the 2014 ImageNet Challenge. The Inception v3 CNN architecture had been proved to be efficient compared with conventional feature-based learning approaches.

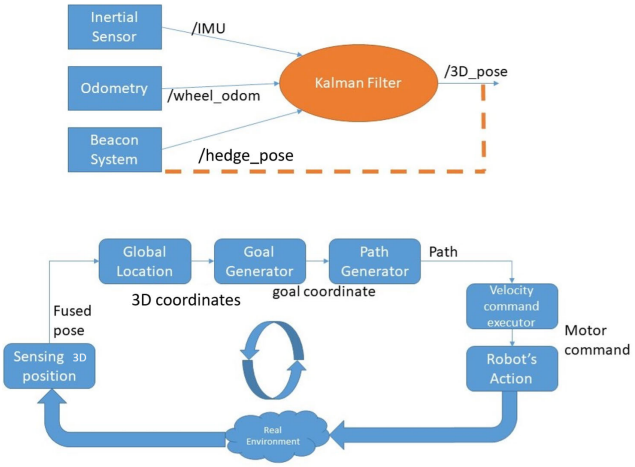

FIGURE 6. Robot localization by sensors fusion and autonomy frame work.

Specifically for transfer learning in our system, the last layer from the Inception v3 model [31] is removed and retrained with our collected dataset. The trained model output will yield the percentage of cleanliness by utilizing the input image. We construct the confusion matrix heatmap of the whole robot's cleaned area during the paint stripping process by using the DCNN output percentages, which are the metal surface's cleanliness level. Each image is resized to 299×299 resolution to fit into Inception v3 architecture and enhance the learned features by the ImageNet pre-trained network. Our transfer learning approach is presented in Fig.7.

B. HEATMAP RECONSTRUCTION

We construct the benchmark heatmap of the robot cleaned area during the paint stripping process by utilizing the surface cleanliness level percentages from the DCNN output. The benchmarking algorithm we proposed here is described in Algorithm 1. The algorithm needs the input odometry data P_t, length of the robot w_R, and the camera's image frames. While the robot is undergoing the paint stripping process, all the probabilities of surface cleanliness levels obtained from deep neural networks are added to construct the benchmarking heatmap. Fig.8 describes the idea behind the benchmarking algorithm. With the help of knowledge from robot odometry data, each cell c_n in Fig.8a can be constructed by calculating the average of all the probabilities of metal surface cleanliness level within the robot navigation from $P_t{}'$ to P_t where the difference of $P_t{}'$ to P_t can be decided by the length of the robot w_R as shown in Fig 8b.

V. EXPERIMENTATION AND RESULT

A. EXPERIMENTAL SCENARIO

We evaluated the paint stripping performance of our hornbill robot with the proposed self-evaluating system under three different paint coatings. We conducted the experiments on a real ship metal plate with a similar thickness and a hull's material composition. The considered metal plate had a dimension of 5m in length and 5m in height. The chosen

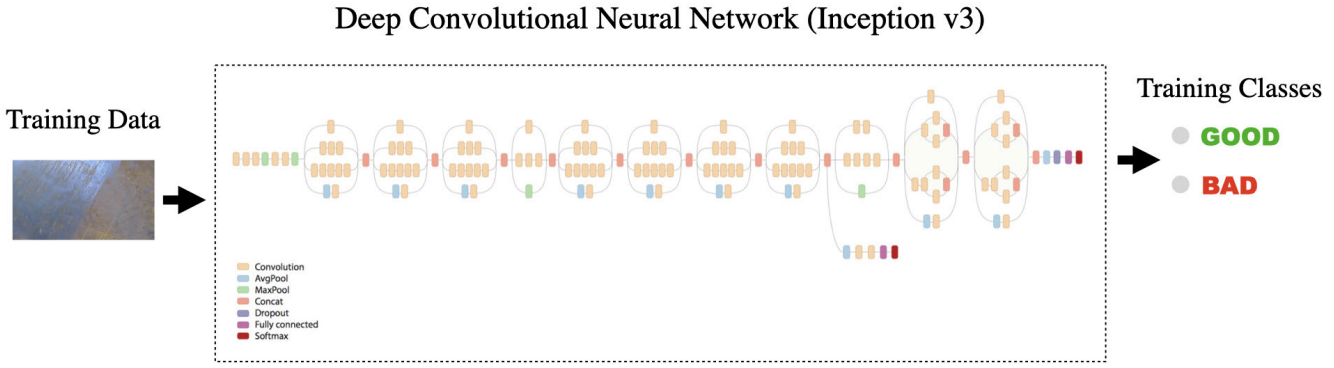

FIGURE 7. Transfer learning using Inception v3.

Algorithm 1 Benchmarking Algorithm Pseudocode

```
procedure Benchmarking(P_t, w_R)
    x̄, X, n ← 0
    P_t' ← P_t
    repeat
        x ← x + probability(Cleanliness)
        n ← n + 1
        if P_t − P_t' > w_R then
            x̄ ← x/n
            add x̄ to X
            x̄, n ← 0
            P_t' ← P_t
        end if
    until zigzag finishes.
    return X
end procedure
```

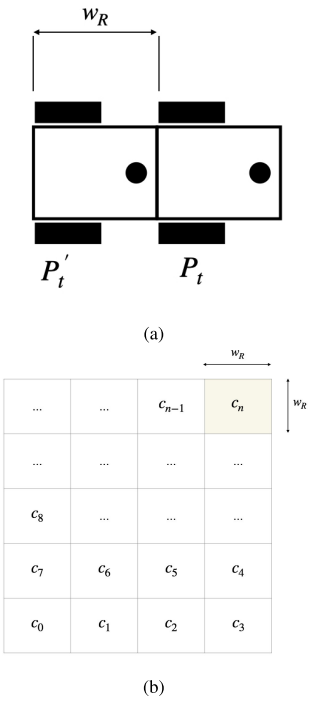

FIGURE 8. Mechanism of benchmarking (a) robot moving from P_t' to P_t (b) heatmap construction.

paint thickness is 0.3 micrometer for paint-I, 0.6 micrometer for paint II, and 1 millimeter for paint III with white color. On a clean plate, we first coat paint and will let it dry for a day, then we start the stripping process with the hornbill robot. Similarly, procedures were followed for the other two paint coatings. Before we start the paint stripping process, the hydro blasting machine with 2500 bar is connected with the robot through the hose. The hose forms the machine to the robot was connected with a mechanical pedal valve, which needs to be pressed manually to release the water. This arrangement was made for safety so that the control person observes the stripping process and releases the valve if any unusual robot behavior is detected. Similarly, the robot's arm movements and nozzle movements will be verified before switching on the water supply. Since we used a small metal plate, the total cleaning distance has been fixed to 3m x 3m. While cleaning the hornbill robot performing the paint stripping process, the camera at the back of the robot would capture the cleaned area and generate a parallel heat map. Fig.9 illustrates the hornbill robot's paint stripping process on the metal plate.

B. DATA COLLECTION AND TRAINING

The dataset is collected from the Keppel shipyard in Singapore. The examples of training image in the dataset are presented in Fig.10 To know the ground truth of cleanliness after the paint stripping, the supervised learning approach is used. The captured images were manually labeled to benchmarking categories with support of expert knowledge. The size of the data set is 5550 images. The dataset was randomly divided into two subsets for training and testing in the ratio of 80:20.

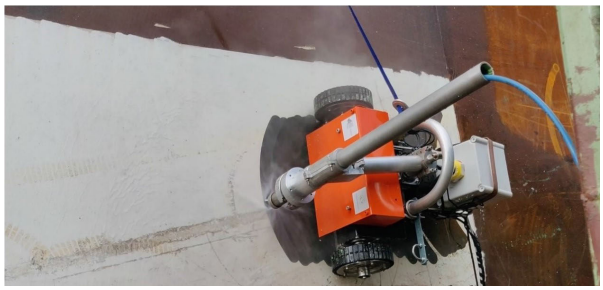

FIGURE 9. Hornbill robot while performing paint stripping process.

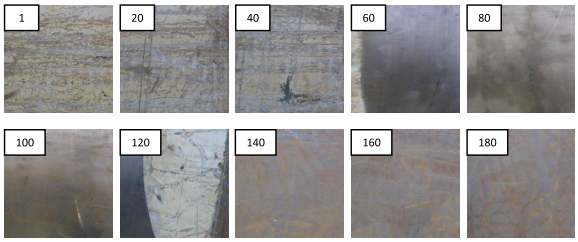

FIGURE 10. Some images in dataset. The number on the image indicate the order of image in the dataset.

To deal with images with image corruptions and real-world images with blurriness, different lighting conditions, we apply online image data augmentation during the training stage. Augmentation is a technique that can be used to artificially expand the size of a training dataset by creating modified versions of images in the dataset. By using shift, flip, brightness, and zoom image, data augmentation techniques can create variations of the images that can improve the fit models' ability to generalize what they have learned to new images.

After loading the trained module in the main processing unit Jetson Xavier, the images steamed from the robot camera are classified with cleanliness probabilities. The probabilities of surface cleanliness levels obtained within the predefined cell are added up in order to construct the benchmarking heatmap.

C. RESULTS AND DISCUSSIONS

Once the position of the robot is fixed, the operator would press the autonomy button, and then the robot starts the stripping process. During the process, the robot parallelly executes the self-evaluating scheme to generate the cleanliness heat map. The robot was navigated autonomously in a zigzag path for the whole paint stripping process with a blasting pressure of 2500 Bar. During the operation, our trained DCNN model is operated in realtime to classify the input images. Our experimented camera operates at 30fps, which is reasonable for running the neural network in realtime. Robot odometry is available through localization services.

Fig. 11 shows the testbed setting where realtime monitor the robot location and benchmarking output while the robot is moving on the ship hull surface. As one can observe,

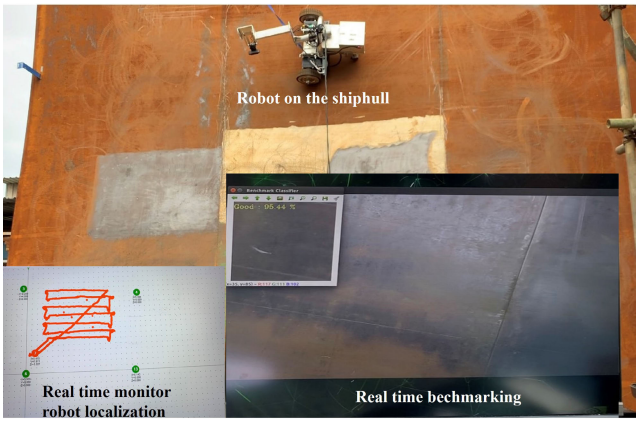

FIGURE 11. Testbed seting with robot localization and benchmarking.

the robot accomplished the movement following the zigzag trajectory then returned to the original position with an offset value of about 0.1 m. The scattered dots plotted along the zigzag trajectory indicate the noise as a kidnapping issue of the UWB beacon location. This proves that the localization system by fusion multiple inputs from the beacon, wheel encoder, and IMU guarantees the robot positions on the ship surface. According to the proposed algorithm 1, the length of the robot L_R is selected as 0.785m by knowing the knowledge of hardware system design. Each 0.785m, an image frame is selected in order to construct the heat map.

Fig.12 represents the tested workspace heatmap images while robot moving on the ship hull surface as Fig.11 for all three considered scenarios. The distance between each heatmap cell is the length of the robot L_R, and each cell represents the probability of the surface cleanliness level output from DCNN. The more the area is clean, the higher the probability of the cell. As mentioned earlier in the first experiment, we tested the surface's cleanliness after removing the paint with a coating level of 0.3 micrometer. The Fig.12a illustrates the generated heat map of the first experiment. We can notice that most of the area was classified as a high probability, which means more clean. The subsequent images Fig.12b and Fig.12c emphasize the value of each cell and the cleaned area of the whole workspace respectively. Since the paint's coated thickness is considerably small, the given hydro blasting pressure should have no issue in removing the layer. Also, the generated heat map from the proposed scheme asserted the same.

In the second experiment, we painted the metal surface with a thick coat of 0.6 micrometer for the same area as previously. We let the paint dry for two days then we started the blasting process. We followed similar procedures as in the first experiment. Fig.12d interprets the cleanliness of the plate, Fig.12e, and Fig.12f depicts the values of each cell with darker uncleaned areas. Interestingly in the second experiment, due to the higher thickness level, We have a darker part in the generated heat map. Usually, with 2500 Bar, the system should remove most of the paint; however, the cleaning

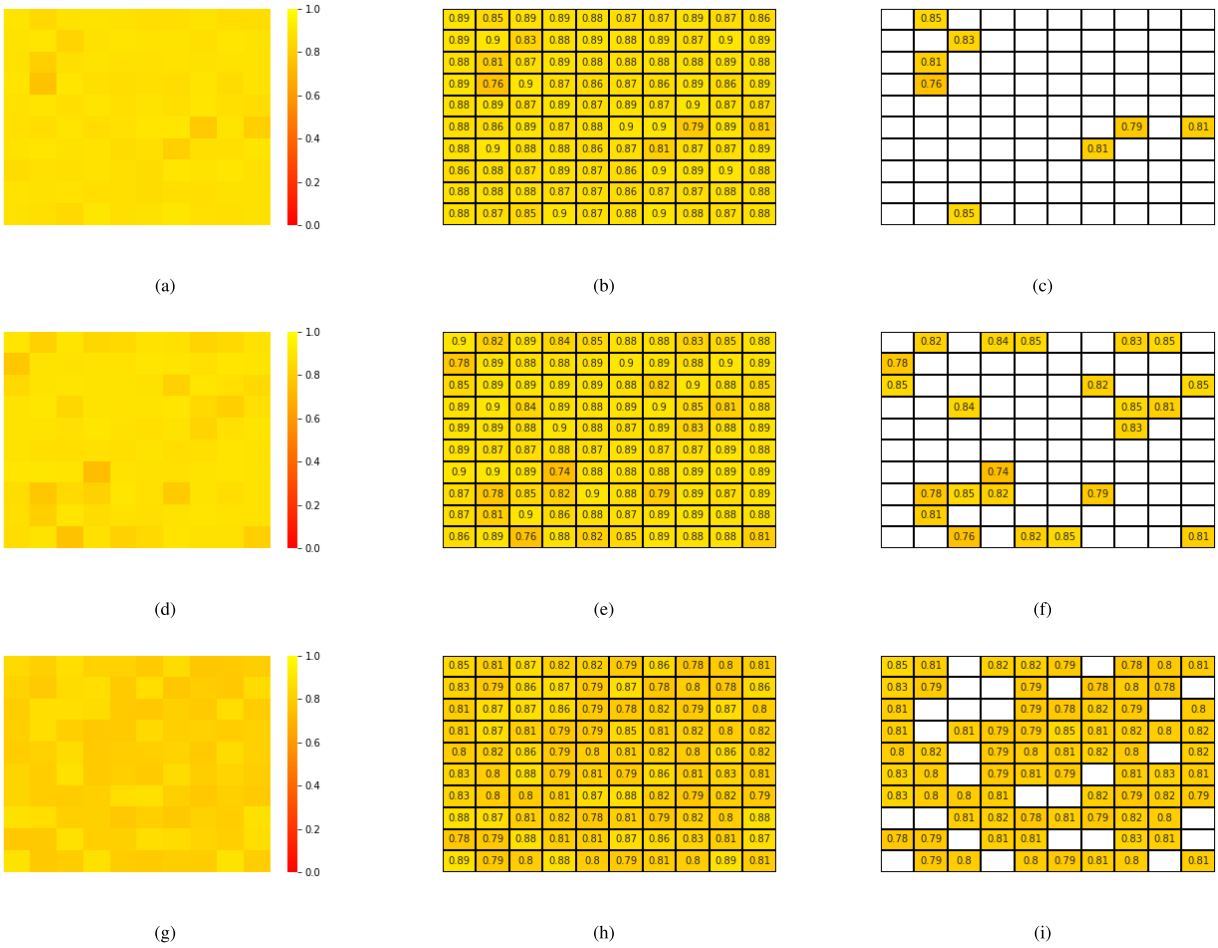

FIGURE 12. Heatmaps for 10 × 10 workspaces with different level of cleanliness (a) (b) (c) are the heatmaps, cell probabilities and thresholded results of the well clean. (d) (e) (f) are the heatmaps, cell probabilities and thresholded results of the moderate clean. (g) (h) (i) are the heatmaps, cell probabilities and thresholded results of the non-clean.

efficiency was reduced due to the nozzle size and distance from the plate. The proposed system successfully generated the heat map that exactly demonstrates the inefficiency of the cleaning process.

Finally, in the last experiment, we used the paint with a coating thickness of 1 mm, and all other procedures were followed as previous. The heats map were generated at the end of the experiment Fig.12g, 12h, and 12i shows the dirty level of the plate. Since the plate's thickness is much higher, the water jet's pressure is not enough to clear the full paint layer. The generated heat map exhibits the same with more number of darker regions. Some places are classified as the fully cleaned region due to some localization error; the robot spent more time blasting in the same place.

The accuracy of the proposed classifier is 95.16%, which is highly adequate for the application context. In addition to miss classification errors, the robot's navigation errors due to localization instability cause errors in synthesizing a heat map. Therefore, the accuracy of navigation and localization of the self-evaluating robot should be maintained at a higher level to minimize the induce of errors.

The maximum robot speed is set to 0.2 m/s and is relatively slow so that the impact of jitter in acquiring image due to robotic movement leading to blurriness is small. On the other hand, since we applied the image compression with a random ratio to the training images during data augmentation, most blurred inputs can still be classified by the trained DCNN model. In case the misclassification by the blur, since the heat map is the average of all probability of all classified images captured when the robot moves within the square cell inside the predefined workspace, so does the effect of the misclassification of the low-quality image are reduced significantly.

The heatmap generated by the robot can be used to ensure the quality of a blasted ship hull before starting the painting. If the paint were applied to a ship hull that was not adequately blasted, the new paint would not last long, which degrades the maintenance work quality. Thereby, the proposed method for synthesizing a self-evaluating map for hydro blasting would

help identify the areas that were not adequately blasted, and subsequently, selective spot blasting could be carried out on those areas. The heat map would be useful in planning an efficient path for the blasting robot for the reblasting process in such cases. Furthermore, the representation of blasting quality categories in the map could decide the amount of pressure required to reblast the corresponding area. For example, if the heat map category is medium, a medium level of pressure can be used. In contrast, if the heat map category of an area is bad, then a high level of pressure can be applied for the corresponding area. Moreover, the categorical representation of the blasting quality in the self-evaluation map would improve the blasting work's overall efficiency. Therefore, the ability to synthesize the self-evaluating map for hydro blasting work on a ship hull is widely useful for improving ship hull maintenance's efficiency and quality.

VI. CONCLUSION

In this paper, we have presented a novel self-evaluating ship hull paint stripping robot called Hornbill. We introduced the mechanical design, system architecture, and the autonomy navigation of the hornbill robot along with the DCNN image classifier module. The proposed image classifier differentiates the hydro blasted surface cleanliness and passes the information to the next stage to generate the heatmap. The generated heat map depicts the cleanliness of the metal surface. Experiments were performed on a metal plate under three different paint coatings to evaluate the proposed self-evaluating scheme's performance. The hornbill robot was performed the paint stripping process autonomously, and eventually, the heatmap was generated. In all three experiments, the proposed self-evaluating could successfully classify the metal plate's cleanliness with an accuracy of 90%. Also, the generated heat maps exactly depicted the dirtiness of the metal plate. With the proposed robot, we are breaking both the manual cleaning and inspection process, which improves the overall efficiency and productivity of ship hull maintenance tasks during dry-docking. There were few drawbacks in the proposed system that affect the system's performance, including the deposit of small water particles on the camera lens and ambient surrounding light's intensity. In the next robot version, we plan to make the chamber with a stable condition to house the perception module and guarantee the light with consistent brightness conditions. The online benchmarking mechanism during paint stripping will also be considered in the future design.

REFERENCES

[1] B. Ramalingam, A. Lakshmanan, M. Ilyas, A. Le, and M. Elara, "Cascaded machine-learning technique for debris classification in floor-cleaning robot application," *Appl. Sci.*, vol. 8, no. 12, p. 2649, Dec. 2018.

[2] A. K. Lakshmanan, R. E. Mohan, B. Ramalingam, A. V. Le, P. Veerajagadeshwar, K. Tiwari, and M. Ilyas, "Complete coverage path planning using reinforcement learning for tetromino based cleaning and maintenance robot," *Autom. Construct.*, vol. 112, Apr. 2020, Art. no. 103078.

[3] A. V. Le, A. A. Hayat, M. R. Elara, N. H. K. Nhan, and K. Prathap, "Reconfigurable pavement sweeping robot and pedestrian cohabitant framework by vision techniques," *IEEE Access*, vol. 7, pp. 159402–159414, 2019.

[4] L. Yi, A. Vu Le, A. A. Hayat, C. S. C. S. Borusu, R. E. Mohan, N. H. K. Nhan, and P. Kandasamy, "Reconfiguration during locomotion by pavement sweeping robot with feedback control from vision system," *IEEE Access*, vol. 8, pp. 113355–113370, 2020.

[5] *AUV Market Research Report*. Accessed: Oct. 22, 2020. [Online]. Available: https://www.researchnester.com/reports/offshore-auv-and-rov-market/1278l

[6] H. Kang, Y.-J. Ham, and J.-S. Oh, "Position estimation method based on the optical displacement sensor for an autonomous hull cleaning robot," *J. Korea Inst. Inf. Commun. Eng.*, vol. 20, no. 2, pp. 385–393, Feb. 2016.

[7] M. H. Lee, K. S. Lee, W. C. Park, S. H. Lee, S. Hong, H. G. Park, J. W. Choi, and H. H. Chun, "On the synthesis of an underwater ship hull cleaning robot system," *Int. J. Precis. Eng. Manuf.*, vol. 13, no. 11, pp. 1965–1973, Nov. 2012.

[8] K. Cassee, "Wheel slip and orientation drift correction for the relative localization system of a ship hull cleaning robot," TU Delft Mech., Maritime Mater. Eng., TU Delft Delft Center Syst. Control, Delft, The Netherlands, Tech. Rep. 2023-04-18, 2018.

[9] B. Steensma, "Ship hull cleaning robots: Obstacle detection using a forward looking sonar system," TU Delft Mech., Maritime Mater. Eng., TU Delft Biomech. Eng., Delft, The Netherlands, Tech. Rep. 2023-02-23, 2018.

[10] D. Souto, A. Faina, F. Lopez-Pena, and R. J. Duro, "Lappa: A new type of robot for underwater non-magnetic and complex hull cleaning," in *Proc. IEEE Int. Conf. Robot. Autom.*, May 2013, pp. 3409–3414.

[11] K. P. Cheng, R. E. Mohan, N. H. Khanh Nhan, and A. V. Le, "Multi-objective genetic algorithm-based autonomous path planning for hinged-tetro reconfigurable tiling robot," *IEEE Access*, vol. 8, pp. 121267–121284, 2020.

[12] M. A. V. J. Muthugala, A. V. Le, E. S. Cruz, M. R. Elara, P. Veerajagadheswar, and M. Kumar, "A self-organizing fuzzy logic classifier for benchmarking robot-aided blasting of ship hulls," *Sensors*, vol. 20, no. 11, p. 3215, Jun. 2020.

[13] Z. Xu, Y. Xie, K. Zhang, Y. Hu, X. Zhu, and H. Shi, "Design and optimization of a magnetic wheel for a grit-blasting robot for use on ship hulls," *Robotica*, vol. 35, no. 3, pp. 712–728, Mar. 2017.

[14] W. Song, H. Jiang, T. Wang, D. Ji, and S. Zhu, "Design of permanent magnetic wheel-type adhesion-locomotion system for water-jetting wall-climbing robot," *Adv. Mech. Eng.*, vol. 10, no. 7, 2018, Art. no. 1687814018787378.

[15] A. Iborra, J. A. Pastor, D. Alonso, B. Alvarez, F. J. Ortiz, P. J. Navarro, C. Fernández, and J. Suardiaz, "A cost-effective robotic solution for the cleaning of ships' hulls," *Robotica*, vol. 28, no. 3, pp. 453–464, May 2010.

[16] A. M. Kabir, J. D. Langsfeld, C. Zhuang, K. N. Kaipa, and S. K. Gupta, "Automated learning of operation parameters for robotic cleaning by mechanical scrubbing," in *Proc. Mater., Biomanufacturing, Properties, Appl. Syst., Sustain. Manuf.*, Jun. 2016, Art. no. V002T04A001.

[17] J. Yin, K. G. S. Apuroop, Y. K. Tamilselvam, R. E. Mohan, B. Ramalingam, and A. V. Le, "Table cleaning task by human support robot using deep learning technique," *Sensors*, vol. 20, no. 6, p. 1698, Mar. 2020.

[18] A. M. Kabir, J. D. Langsfeld, S. Shriyam, V. S. Rachakonda, C. Zhuang, K. N. Kaipa, J. Marvel, and S. K. Gupta, "Planning algorithms for multi-setup multi-pass robotic cleaning with oscillatory moving tools," in *Proc. IEEE Int. Conf. Autom. Sci. Eng. (CASE)*, Aug. 2016, pp. 751–757.

[19] P. Veerajagadheswar, K. Ping-Cheng, M. R. Elara, A. V. Le, and M. Iwase, "Motion planner for a tetris-inspired reconfigurable floor cleaning robot," *Int. J. Adv. Robotic Syst.*, vol. 17, no. 2, 2020, Art. no. 1729881420914441.

[20] A. Le, V. Prabakaran, V. Sivanantham, and R. Mohan, "Modified a-star algorithm for efficient coverage path planning in tetris inspired self-reconfigurable robot with integrated laser sensor," *Sensors*, vol. 18, no. 8, p. 2585, Aug. 2018.

[21] A. Le, P.-C. Ku, T. Than Tun, N. Huu Khanh Nhan, Y. Shi, and R. Mohan, "Realization energy optimization of complete path planning in differential drive based self-reconfigurable floor cleaning robot," *Energies*, vol. 12, no. 6, p. 1136, Mar. 2019.

[22] A. V. Le, N. H. K. Nhan, and R. E. Mohan, "Evolutionary algorithm-based complete coverage path planning for tetriamond tiling robots," *Sensors*, vol. 20, no. 2, p. 445, Jan. 2020.

[23] A. Manimuthu, A. V. Le, R. E. Mohan, P. Veerajagadeshwar, N. H. K. Nhan, and K. P. Cheng, "Energy consumption estimation model for complete coverage of a tetromino inspired reconfigurable surface tiling robot," *Energies*, vol. 12, no. 12, p. 2257, Jun. 2019.

[24] W. Hess, D. Kohler, H. Rapp, and D. Andor, "Real-time loop closure in 2D LIDAR SLAM," in *Proc. IEEE Int. Conf. Robot. Autom. (ICRA)*, May 2016, pp. 1271–1278.
[25] C. Kerl, J. Sturm, and D. Cremers, "Dense visual SLAM for RGB-D cameras," in *Proc. IEEE/RSJ Int. Conf. Intell. Robots Syst.*, Nov. 2013, pp. 2100–2106.
[26] A. V. Le, R. Parween, R. Elara Mohan, N. H. K. Nhan, and R. Enjikalayil Abdulkader, "Optimization complete area coverage by reconfigurable hTrihex tiling robot," *Sensors*, vol. 20, no. 11, p. 3170, Jun. 2020.
[27] A. V. Le and J. Choi, "Robust tracking occluded human in group by perception sensors network system," *J. Intell. Robotic Syst.*, vol. 90, nos. 3–4, pp. 349–361, Jun. 2018.
[28] M. Quigley, K. Conley, B. Gerkey, J. Faust, T. Foote, J. Leibs, R. Wheeler, and A. Y. Ng, "ROS: An open-source robot operating system," in *Proc. ICRA Workshop Open Source Softw.*, Kobe, Japan, vol. 3, no. 3.2, 2009, p. 5.
[29] L. D'Alfonso, W. Lucia, P. Muraca, and P. Pugliese, "Mobile robot localization via EKF and UKF: A comparison based on real data," *Robot. Auto. Syst.*, vol. 74, pp. 122–127, Dec. 2015.
[30] Y. Shi, M. R. Elara, A. V. Le, V. Prabakaran, and K. L. Wood, "Path tracking control of self-reconfigurable robot hTetro with four differential drive units," *IEEE Robot. Autom. Lett.*, vol. 5, no. 3, pp. 3998–4005, Jul. 2020.
[31] C. Szegedy, V. Vanhoucke, S. Ioffe, J. Shlens, and Z. Wojna, "Rethinking the inception architecture for computer vision," in *Proc. IEEE Conf. Comput. Vis. Pattern Recognit. (CVPR)*, Jun. 2016, pp. 2818–2826.
[32] O. Russakovsky, J. Deng, H. Su, J. Krause, S. Satheesh, S. Ma, Z. Huang, A. Karpathy, A. Khosla, M. Bernstein, A. C. Berg, and L. Fei-Fei, "ImageNet large scale visual recognition challenge," *Int. J. Comput. Vis.*, vol. 115, no. 3, pp. 211–252, Dec. 2015.
[33] S. J. Pan and Q. Yang, "A survey on transfer learning," *IEEE Trans. Knowl. Data Eng.*, vol. 22, no. 10, pp. 1345–1359, Oct. 2010.

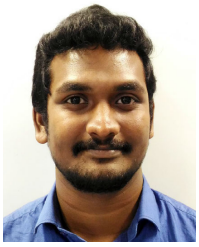

VEERAJAGADHESWAR PRABAKARAN received the bachelor's degree in electronics and instrumentation engineering from Sathyabama University, India, in 2013, and the Ph.D. degree in advanced engineering from Tokyo Denki University, in 2019. He is currently working as a Research Fellow with the ROARS Laboratory, Singapore University of Technology and Design. He is also a Visiting Instructor for a design course with the International Design Institute, Zhejiang University, China. His research interests include the development of complete coverage path planning, SLAM framework and embedded control for reconfigurable, and climbing robots. He received the SG Mark Design Award, in 2017, for the designing of h-Tetro, a self-reconfigurable cleaning robot.

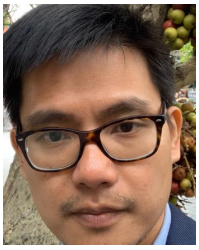

ANH VU LE received the B.S. degree in electronics and telecommunications from the Hanoi University of Technology, Vietnam, in 2007, and the Ph.D. degree in electronics and electrical from Dongguk University, South Korea, in 2015. He is currently with the Opto-electronics Research Group, Faculty of Electrical and Electronics Engineering, Ton Duc Thang University, Ho Chi Minh City, Vietnam. He is also a Postdoctoral Research Fellow with the ROAR Laboratory, Singapore University of Technology and Design. His current research interests include robotics vision, robot navigation, human detection, action recognition, feature matching, and 3D video processing.

PHONE THIHA KYAW is currently pursuing the B.E. degree in mechatronics with Yangon Technological University. He is also working as a Visit Fellow with the Robotics and Automation Research Laboratory (ROAR), Singapore University of Technology and Design. He participated in many different robotic competitions, including First Global Challenge 2017, which was held in Washington DC, and his Team Myanmar achieved rank 6 out of 163 teams. His research interests include autonomous robots, sensor fusion systems, control engineering, and computer vision applications.

RAJESH ELARA MOHAN received the B.E. degree from Bharathiar University, India, in 2003, and the M.Sc. and Ph.D. degrees from Nanyang Technological University, in 2005 and 2012, respectively. He is currently an Assistant Professor with the Engineering Product Development Pillar, Singapore University of Technology and Design (SUTD). He is also a Visiting Faculty Member of the International Design Institute, Zhejiang University, China. He has published more than 80 papers in leading journals, books, and conferences. His research interests include robotics with an emphasis on self-reconfigurable platforms as well as research problems related to robot ergonomics and autonomous systems. He was a recipient of the SG Mark Design Award, in 2016 and 2017, the ASEE Best of Design in Engineering Award, in 2012, and the Tan Kah Kee Young Inventors' Award, in 2010.

PRATHAP KANDASAMY received the B.Sc. degree in computer engineering from the Singapore University of Technology and Design, in 2010. He is currently working as a Research Officer with the Engineering Product Development Pillar, Singapore University of Technology and Design. His research interest includes mechanical design.

TAN NHAT NGUYEN (Member, IEEE) received the B.S. and M.S. degrees in electronics and telecommunications engineering from the Ho Chi Minh University of Natural Sciences, a member of Vietnam National University, Ho Chi Minh City, Vietnam, in 2008 and 2012, respectively, and the Ph.D. degree in computer science, communication technology and applied mathematics from the VSB Technical University of Ostrava, Czech Republic, where he is currently pursuing the Ph.D. degree in electrical engineering. He joined the Faculty of Electrical and Electronics Engineering, Ton Duc Thang University, Vietnam, in 2013. Since 2013, he has been working as a Lecturer with Ton Duc Thang University. His major research interests include robotics vision and image processing.

MADHUKUMAR KANNAN is currently the Cofounder and the Director of Oceania Robotics Pte. Ltd. He is also the Director of Brightsun Electricals, an established company whose principal activity is building and repairing of ships, tankers and other ocean-going vessels, including conversion of ships into off-shore structures with wholesale of electrical and wiring accessories as the secondary activity. He is responsible for the overall management and day-to-day operations of both the companies as well as the formulation of the business directions, strategies and policies of the wider Brightsun Group.